

# Cosmological-Model-Parameter Determination from Satellite-Acquired Type Ia and IIP Supernova Data

Silviu Podariu<sup>1</sup>, Peter Nugent<sup>2</sup>, and Bharat Ratra<sup>1</sup>

## ABSTRACT

We examine the constraints that satellite-acquired Type Ia and IIP supernova apparent magnitude versus redshift data will place on cosmological model parameters in models with and without a constant or time-variable cosmological constant  $\Lambda$ . High-quality data which could be acquired in the near future will result in tight constraints on these parameters. For example, if all other parameters of a spatially-flat model with a constant  $\Lambda$  are known, the supernova data should constrain the non-relativistic matter density parameter  $\Omega_0$  to better than 1% (2%, 0.5%) at  $1\sigma$  with neutral (worst case, best case) assumptions about data quality.

*Subject headings:* cosmology: observation—large-scale structure of the universe—space vehicles—supernovae: general

## 1. Introduction

Recent applications of the apparent magnitude versus redshift test based on Type Ia supernovae (hereafter SNe Ia) have resulted in interesting constraints on cosmological-model parameters (see, e.g., Riess et al. 1998; Perlmutter et al. 1999; Podariu & Ratra 2000; Waga & Frieman 2000; Gott et al. 2000). Higher quality SN Ia and SN IIP data will result in tighter constraints on cosmological-model parameters. A dedicated SN space telescope should provide the high quality data needed to realize the full potential of this neoclassical cosmological test.

In this paper we examine constraints on cosmological-model parameters that will result from such a data set. For definiteness we focus on data that could be acquired by the proposed SNAP space telescope (Curtis et al. 2000 and <http://snap.lbl.gov>). That is, we assume a data set of 2000 SNe Ia multi-frequency light curves, possibly augmented with 10,000 SNe IIP multi-frequency light curves, for SNe out to redshift  $z = 2$ , with errors discussed below.

---

<sup>1</sup>Department of Physics, Kansas State University, Manhattan, KS 66506.

<sup>2</sup>Lawrence Berkeley National Laboratory, MS50-232, 1 Cyclotron Road, Berkeley, CA 94720.

Observational data favor models with a low  $\Omega_0$ . The simplest such models have either flat spatial hypersurfaces and a constant or time-variable cosmological “constant”  $\Lambda$  (see, e.g., Peebles 1984; Peebles & Ratra 1988; Sahni & Starobinsky 2000; Steinhardt 1999; Carroll 2000; Binétruy 2000), or open spatial hypersurfaces and no  $\Lambda$  (see, e.g., Gott 1982, 1997; Ratra & Peebles 1994, 1995; Kamionkowski et al. 1994; Górski et al. 1998). For a constant  $\Lambda$  (with density parameter  $\Omega_\Lambda$ ), these models lie along the lines  $\Omega_0 + \Omega_\Lambda = 1$  and  $\Omega_\Lambda = 0$ , respectively, in the more general two-dimensional  $(\Omega_0, \Omega_\Lambda)$  model-parameter space. Depending on the values of  $\Omega_0$  and  $\Omega_\Lambda$ , models in this two-dimensional parameter space have either closed, flat, or open spatial hypersurfaces. In this paper we derive constraints on the parameters of the two-dimensional model as well as those of the special one-dimensional cases.

We also derive constraints on the parameters of a spatially-flat model with a time-variable  $\Lambda$ . The only known consistent model for a time-variable  $\Lambda$  is that based on a scalar field ( $\phi$ ) with a scalar field potential  $V(\phi)$  (Ratra & Peebles 1988). In this paper we focus on the favored model which at low  $z$  has  $V(\phi) \propto \phi^{-\alpha}$ ,  $\alpha > 0$  (Peebles & Ratra 1988; Ratra & Peebles 1988)<sup>3</sup>. This model is in reasonable accord with observational data (see, e.g., Peebles & Ratra 1988; Ratra & Quillen 1992; Podariu & Ratra 2000; Waga & Frieman 2000; Brax, Martin, & Riazuelo 2000)<sup>4</sup>.

A scalar field is mathematically equivalent to a fluid with a time-dependent speed of sound (Ratra 1991), and it may be shown that with  $V(\phi) \propto \phi^{-\alpha}$ ,  $\alpha > 0$ , the  $\phi$  energy density behaves like a cosmological constant that decreases with time. We emphasize that in our analysis of this model here we do not make use of the time-independent equation of state fluid approximation to the model that has sometimes been used for such computations (see the discussion in Podariu & Ratra 2000).

Huterer & Turner (1999), Starobinsky (1998), Nakamura & Chiba (1999), Saini et al. (2000), and Chiba & Nakamura (2000) discuss using SN apparent magnitude versus redshift data to determine the scalar field potential of the time-variable  $\Lambda$  model. This is a difficult task. Maor, Brustein, & Steinhardt (2000) note that even data of the quality anticipated from SNAP will not result in very tight constraints on an arbitrary equation of state. They consider a simple illustrative example, with an equation of state parameter  $w$  that has two terms, one constant and the other linear in  $z$ . Maor et al. show confidence contours (in a two-dimensional plane) for the two parameters in the equation of state for this model in their Figure 2. After marginalizing over  $\Omega_0$  the peak-to-peak spread in their  $2\sigma$  contour for the equation of state at  $z = 0$ ,  $w_0$ , is about  $-0.3$  for  $w_0 = -0.7$ ,

---

<sup>3</sup>Such a scalar field potential is present in some high energy particle physics models (see, e.g., Rosati 2000; Copeland, Nunes, & Rosati 2000; Brax & Martin 2000). Fujii (2000), Cormier & Holman (2000), Faraoni (2000), Baccigalupi, Perrotta, & Matarrese (2000), Dodelson, Kaplinghat, & Stewart (2000), Ziaeeepour (2000), Kruger & Norbury (2000), Joyce & Prokopec (2000), Goldberg (2000), Hebecker & Wetterich (2000), Ureña-López & Matos (2000), and Armendariz-Picon, Mukhanov, & Steinhardt (2000) discuss this model and other options.

<sup>4</sup>See, e.g., Vishwakarma (2000), Ng & Wiltshire (2000), and Lima & Alcaniz (2000) for observational constraints on related models.

or about 43% of the value of  $w_0$ . This corresponds to a symmetrized  $2\sigma$  uncertainty of about  $\pm 22\%$  on  $w_0$ <sup>5</sup>. The corresponding peak-to-peak spread in their  $1\sigma$  contour is about  $-0.22$ , which corresponds to a  $1\sigma$  uncertainty of about  $\pm 16\%$  on  $w_0$ . For fixed  $\Omega_0$ , the peak-to-peak spread in their  $1\sigma$  contour is about  $-0.09$ , which corresponds to a  $1\sigma$  uncertainty of about  $\pm 6.5\%$  on  $w_0$ . While much larger than the constraints we place on model-parameter values (see below) this is still a reasonably precise determination of  $w_0$ .

Motivated by the approach adopted in analyses of current SN apparent magnitude versus redshift data (see, e.g., Riess et al. 1998; Perlmutter et al. 1999), we instead focus on how well future SN data will constrain parameters of various cosmological models<sup>6</sup>.

We want to determine how well SN data distinguishes between different cosmological-model-parameter values. To do this we pick a model and a range of model-parameter values and compute the luminosity distance  $D_L(z)$  for a grid of model-parameter values that span this range. Figure 1 shows examples of  $D_L(z)$ ’s computed in the time-variable  $\Lambda$  model (Peebles & Ratra 1988).

The error bars on the SN fluxes are the ones that are most likely to be symmetric (and thus allow for the simplest comparison between model predictions and observational data), so we work with flux  $f \propto D_L^{-2}$  for the comparison between model predictions and anticipated data. For our purposes, the constant of proportionality in this relation is unimportant since the SNe in the final reduced data set have been made standardized candles (see, e.g., Phillips 1993, and more recently Riess et al. 1998; Perlmutter et al. 1999).

For computational simplicity we assume SN data from SNAP will be combined to provide fluxes and errors on fluxes for 67 uniform bins in redshift, of width  $\Delta z = 0.03$ , with the first one centered at  $z = 0.03$  and the last one at  $z = 2.01$ . In each bin the statistical and systematic errors are combined to give a flux error distribution with standard deviation  $\sigma(z)$ . With 2000 SNe Ia and 10,000 SNe IIP  $\sigma(z)$  is estimated to be 2% in each redshift bin up to  $z = 1.7$ , and then increasing linearly with redshift to 10% at  $z = 2$ . This is the “neutral” case. The “best” case assumes that errors are limited by  $\sqrt{N}$  statistics (with systematic errors at or below the 1% level), giving  $\sigma(z) = 1\%$  over the whole redshift range. The “worst” case (with SNe Ia only — this is the baseline mission) assumes  $\sigma(z) = 3\%$  to  $z = 1.2$  and  $= 10\%$  from  $z = 1.2$  to  $z = 2$ .

Currently a single SN Ia provides a  $\approx 16\%$  measurement of the flux ( $\approx 8\%$  in distance) (Jha et al. 1999). A large fraction of this uncertainty almost certainly resides in the correction for

---

<sup>5</sup>We acknowledge helpful discussions with P. Steinhardt on this issue.

<sup>6</sup>A similar approach is used in analyses of cosmic microwave background anisotropy data. Here one computes predictions of a theoretical model as a function of a few cosmological parameters and derives constraints on these parameters by comparing these predictions to observational data, either using an approximate  $\chi^2$  technique (see, e.g., Ganga, Ratra, & Sugiyama 1996; Dodelson 2000; Le Dour et al. 2000; Lange et al. 2000; Balbi et al. 2000), or using the complete models-based maximum likelihood technique (see, e.g., Ganga et al. 1997, 1998; Ratra et al. 1998, 1999; Rocha et al. 1999).

extinction. By going to space one will be able to greatly increase the wavelength coverage and precision of the photometric measurements, thereby reducing this uncertainty considerably. A conservative estimate of the intrinsic uncertainty for a given SN Ia with this type of data set would be  $\approx 10\%$  in flux ( $\approx 5\%$  in distance). There is potential for reducing this even further through the identification of additional parameters that constrain the corrected peak luminosity of SNe Ia beyond the single parameter of light-curve shape currently used.

A major advantage of a space telescope is the much better opportunity for controlling (or studying) the many known (and unknown) sources of error. These include environmental effects, evolution, intergalactic dust, unusual cases which bias the distribution, etc. See, e.g., Howell, Wang, & Wheeler (2000), Aldering, Knop, & Nugent (2000), Croft et al. (2000), Nomoto et al. (2000), Barber (2000), Hamuy et al. (2000), Livio (2000), Totani (2000), and Gott et al. (2000) for discussions of some of these issues. Without understanding and limiting these sources of error an accurate measurement of the cosmological parameters can not be obtained.

The potential value of SNe IIP as distance indicators is considerable. For a space telescope search that will discover  $\approx 2000$  SNe Ia a conservative estimate (based on the local rates) of the number of SNe IIP discovered would be  $\approx 10,000$ . This number greatly increases if one takes account of the increase in the star formation rate at higher  $z$  (for discussions of the rates of SNe discovered at high- $z$ , via HST, see Sullivan et al. 2000 and Gilliland, Nugent, & Phillips 1999). Eastman, Schmidt, & Kirshner (1996) have shown how the use of the expanding photosphere method (EPM) can yield reliable distances ( $\approx 15\%$ ) to well observed SNe IIP. While SNAP will obtain high-quality, multi-frequency light curves for these objects, obtaining the necessary spectra for all these SNe goes well beyond the current SNAP mission. However, spectra for many of them will be obtained by SNAP and the potential for obtaining spectra via other sources (large ground-based telescopes with adaptive optics and/or NGST) could lead to several hundred or thousand SNe IIP with good EPM distances. In addition, there may exist other methods to derive cruder distances to SNe IIP based solely on their light curves (see, e.g., Höflich et al. 2000; Young 1994). Here one would be able to use almost all of the photometrically observed SNe IIP and rely on  $\sqrt{N}$  statistics to beat down the larger uncertainties.

To determine how well SN data will distinguish between different sets of model-parameter values, we pick a fiducial set of model-parameter values which give a flux  $f_F(z)$  and compute

$$N_\sigma(P) = \sqrt{\sum_{i=1}^{67} \left( \frac{f(P, z_i) - f_F(z_i)}{\sigma(z_i)f_F(z_i)} \right)^2}, \quad (1)$$

where the sum runs over the 67 redshift bins and  $P$  represents the model parameters, for instance  $\Omega_0$  and  $\Omega_\Lambda$  in the general two-dimensional constant  $\Lambda$  case.  $N_\sigma(P)$  is the number of standard deviations the model-parameter set  $P$  lies away from that of the fiducial model. This representation (eq. [1]) is exact for the case where the correlated errors between redshift bins for the distance determinations are negligible.

Results are presented and discussed in the next section and we conclude in §3.

## 2. Results and Discussion

Figure 2 illustrates the ability of anticipated SNAP data to constrain cosmological-model parameters for the general two-dimensional constant  $\Lambda$  case. SNAP data with even worst case error bars will lead to greatly improved cosmological-parameter determination (see, e.g., Riess et al. 1998, Perlmutter et al. 1999, and Podariu & Ratra 2000 for constraints from current data). We note that as expected the contours are elliptical, indicating that one combination of the parameters is better constrained than the other orthogonal combination (see, e.g., Goobar & Perlmutter 1995).

Figure 3 illustrates the ability of SNAP data to distinguish between a constant and a time-variable  $\Lambda$  in a spatially-flat model. The fiducial model here is a constant  $\Lambda$  ( $\alpha = 0$ ) model with  $\Omega_0 = 0.28$  and  $\Omega_\Lambda = 0.72$ . SNAP data with even worst case error bars will result in greatly improved discrimination (see, e.g., Podariu & Ratra 2000 for the current situation). We note again that the contours are elliptical.

Figure 4 illustrates the ability of SNAP data to constrain  $\Omega_0$  and  $\alpha$  in the spatially-flat time-variable  $\Lambda$  model (Peebles & Ratra 1988). Here the time-variable  $\Lambda$  fiducial model has  $\Omega_0 = 0.2$  and  $\alpha = 4$ . Again, SNAP will allow for tight constraints on these cosmological parameters.

If other data (such as cosmic microwave background anisotropy measurements from MAP and Planck Surveyor and weak-lensing studies from the proposed SNAP mission) pinned down some of the cosmological parameters, the SN data would then be able to provide tighter constraints on the remaining parameters. For instance, Figure 5 shows constraints from SNAP data on  $\Omega_0$  in a spatially-flat constant  $\Lambda$  model and in an open  $\Lambda = 0$  model. As expected from the elliptical shape of the contours in Figure 2, anticipated SN data will constrain  $\Omega_0$  more tightly in the spatially-flat case than in the open case. In both cases SNAP will provide tight constraints on  $\Omega_0$ . For instance, at  $3\sigma$ , in the spatially-flat model we find  $\Omega_0 = 0.3 \pm 0.007$ ,  $= 0.3 \pm 0.015$ , and  $= 0.3 \pm 0.003$  for neutral, worst, and best case errors, while in the open model we have  $\Omega_0 = 0.3 \pm 0.015$ ,  $= 0.3 \pm 0.03$ , and  $= 0.3 \pm 0.006$  for neutral, worst, and best case errors.

Figure 6 shows the SNAP data constraints on  $\Omega_0$  and  $\alpha$  in the spatially-flat time-variable  $\Lambda$  model, if other data were to require that either  $\alpha = 4$  or  $\Omega_0 = 0.2$ . SNAP data will provide tight constraints on these parameters. For instance, if  $\alpha = 4$  we find  $\Omega_0 = 0.2 \pm 0.009$ ,  $= 0.2 \pm 0.02$ , and  $= 0.2 \pm 0.004$  for neutral, worst, and best case errors, while if  $\Omega_0 = 0.2$  we have  $\alpha = 4 \pm 0.25$ ,  $= 4 \pm 0.5$ , and  $= 4 \pm 0.1$  for neutral, worst, and best case errors, all at  $3\sigma$ .

### 3. Conclusion

SN space telescope data of the quality assumed here will lead to tight constraints on cosmological-model parameters. For instance, in a spatially-flat constant  $\Lambda$  model where all other parameters are known, anticipated SNAP data will determine  $\Omega_0$  to about  $\pm 0.8\%$ ,  $\pm 1.7\%$ , and  $\pm 0.4\%$  (for neutral, worst, and best case errors respectively) at  $1\sigma$ . The corresponding errors on  $\Omega_0$  for the open case are about  $\pm 1.6\%$ ,  $\pm 3.7\%$ , and  $\pm 0.7\%$ . For the time-variable  $\Lambda$  model, when  $\alpha$  is fixed,  $\Omega_0$  will be known to about  $\pm 1.5\%$ ,  $\pm 3.1\%$ , and  $\pm 0.7\%$ , respectively, while when  $\Omega_0$  is fixed,  $\alpha$  will be determined to about  $\pm 2.2\%$ ,  $\pm 4.2\%$ , and  $\pm 1.2\%$ . This will have important consequences for cosmology.

We acknowledge valuable discussions with G. Aldering, M. Levi, S. Perlmutter, and T. Souradeep. SP and BR acknowledge support from NSF CAREER grant AST-9875031 and PN acknowledges computational support from the DOE Office of Science under Contract No. DE-AC03-76SF00098.

## REFERENCES

- Aldering, G., Knop, R., & Nugent, P. 2000, *AJ*, 119, 2110
- Armendariz-Picon, C., Mukhanov, V., & Steinhardt, P.J. 2000, *astro-ph/0004134*
- Baccigalupi, C., Perrotta, F., & Matarrese, S. 2000, in *COSMO99*, in press
- Balbi, A., et al. 2000, *ApJ*, submitted
- Barber, A.J. 2000, *MNRAS*, submitted
- Binétruy, P. 2000, in *The Early Universe*, in press
- Brax, P., & Martin, J. 2000, in *Energy Densities in the Universe*, in press
- Brax, P., Martin, J., & Riazuelo, A. 2000, *Phys. Rev. D*, submitted
- Carroll, S.M. 2000, *Living Rev. Relativity*, submitted
- Chiba, T., & Nakamura, T. 2000, *astro-ph/0008175*
- Copeland, E.J., Nunes, N.J., & Rosati, F. 2000, *hep-ph/0005222*
- Cormier, D., & Holman, R. 2000, *Phys. Rev. Lett.*, 84, 5936
- Croft, R.A.C., Davé, R., Hernquist, L., & Katz, N. 2000, *ApJ*, submitted
- Curtis, D., et al. 2000, *Supernova / Acceleration Probe (SNAP)*, proposal to DOE and NSF
- Dodelson, S. 2000, *Int. J. Mod. Phys.*, in press
- Dodelson, S., Kaplinghat, M., & Stewart, E. 2000, *Phys. Rev. Lett.*, submitted
- Eastman, R.G., Schmidt, B.P., & Kirshner, R. 1996, *ApJ*, 466, 911
- Faraoni, V. 2000, *Phys. Rev. D*, 62, 023504
- Fujii, Y. 2000, in *Ninth Workshop on General Relativity and Gravitation*, in press
- Ganga, K., Ratra, B., Gundersen, J.O., & Sugiyama, N. 1997, *ApJ*, 484, 7
- Ganga, K., Ratra, B., Lim, M.A., Sugiyama, N., & Tanaka, S.T. 1998, *ApJS*, 114, 165
- Ganga, K., Ratra, B., & Sugiyama, N. 1996, *ApJ*, 461, L61
- Gilliland, R.L., Nugent, P.E., & Phillips, M.M. 1999, *ApJ*, 521, 30
- Goldberg, H. 2000, *hep-ph/0003197*
- Goobar, A., & Perlmutter, S. 1995, *ApJ*, 450, 14

- Górski, K.M., Ratra, B., Stompor, R., Sugiyama, N., & Banday, A.J. 1998, *ApJS*, 114, 1
- Gott, J.R. 1982, *Nature*, 295, 304
- Gott, J.R. 1997, in *Critical Dialogues in Cosmology*, ed. N. Turok (Singapore: World Scientific), 519
- Gott, J.R., Vogeley, M.S., Podariu, S., & Ratra, B. 2000, *astro-ph/0006103*
- Hamuy, M., Trager, S.C., Pinto, P.A., Phillips, M.M., Schommer, R.A., Ivanov, V., and Suntzeff, N.B. 2000, *AJ*, in press
- Hebecker, A., & Wetterich, C. 2000, *hep-ph/0003287*
- Höflich, P., Straniero, O., Limongi, M., Dominguez, I., & Chieffi, A. 2000, *Rev. Mex. AyA*, in press
- Howell, D.A., Wang, L., & Wheeler, J.C. 2000, *ApJ*, 530, 166
- Huterer, D., & Turner, M.S. 1999, *Phys. Rev. D*, 60, 081301
- Jha, S., et al. 1999, *ApJS*, 125, 73
- Joyce, M., & Prokopec, T. 2000, *hep-ph/0003190*
- Kamionkowski, M., Ratra, B., Spergel, D.N., & Sugiyama, N. 1994, *ApJ*, 434, L1
- Kruger, A.T., & Norbury, J.W. 2000, *Phys. Rev. D*, 61, 087303
- Lange, A.E., et al. 2000, *Phys. Rev. D*, submitted
- Le Dour, M., Douspis, M., Bartlett, J.G., & Blanchard, A. 2000, *A&A*, submitted
- Lima, J.A.S., & Alcaniz, J.S. 2000, *MNRAS*, 312, 747
- Livio, M. 2000, in *The Greatest Explosions Since the Big Bang: Supernovae and Gamma-Ray Bursts*, ed. M. Livio, N. Panagia, and K. Sahu, in press
- Maor, I., Brustein, R., & Steinhardt, P.J. 2000, *astro-ph/0007297*
- Nakamura, T., & Chiba, T. 1999, *MNRAS*, 306, 696
- Ng, S.C.C., & Wiltshire, D.L. 2000, *astro-ph/0004138*
- Nomoto, K., Umeda, H., Kobayashi, C., Hachisu, I., Kato, M., & Tsujimoto, T. 2000, in *Cosmic Explosions!*, ed. S.S. Holt and W.W. Zhang (AIP), in press
- Peebles, P.J.E. 1984, *ApJ*, 284, 439
- Peebles, P.J.E., & Ratra, B. 1988, *ApJ*, 325, L17



- Perlmutter, S., et al. 1999, *ApJ*, 517, 565
- Phillips, M.M. 1993, *ApJ*, 413, L105
- Podariu, S., & Ratra, B. 2000, *ApJ*, 532, 109
- Ratra, B. 1991, *Phys. Rev. D*, 43, 3802
- Ratra, B., Ganga, K., Sugiyama, N., Tucker, G.S., Griffin, G.S., Nguyễn, H.T., & Peterson, J.B. 1998, *ApJ*, 505, 8
- Ratra, B., & Peebles, P.J.E. 1988, *Phys. Rev. D*, 37, 3406
- Ratra, B., & Peebles, P.J.E. 1994, *ApJ*, 432, L5
- Ratra, B., & Peebles, P.J.E. 1995, *Phys. Rev. D*, 52, 1837
- Ratra, B., & Quillen, A. 1992, *MNRAS*, 259, 738
- Ratra, B., Stompor, R., Ganga, K., Rocha, G., Sugiyama, N., & Górski, K.M. 1999, *ApJ*, 517, 549
- Riess, A.G., et al. 1998, *AJ*, 116, 1009
- Rocha, G., Stompor, R., Ganga, K., Ratra, B., Platt, S.R., Sugiyama, N., & Górski, K.M. 1999, *ApJ*, 525, 1
- Rosati, F. 2000, in *COSMO99*, in press
- Sahni, V., & Starobinsky, A. 2000, *Int. J. Mod. Phys. D*, 9, 1
- Saini, T.D., Raychaudhury, S., Sahni, V., & Starobinsky, A.A. 2000, *Phys. Rev. Lett.*, 85, 1162
- Starobinsky, A.A. 1998, *JETP Lett.*, 68, 757
- Steinhardt, P.J. 1999, in *Proceedings of the Pritzker Symposium on the Status of Inflationary Cosmology*, in press
- Sullivan, R., Ellis, R., Nugent, P., Smail, I., & Madau, P. 2000, *MNRAS*, in press
- Totani, T. 2000, in *Dark Matter 2000*, in press
- Ureña-López, L.A., & Matos, T. 2000, *astro-ph/0003364*
- Vishwakarma, R.G. 2000, *gr-qc/9912105*
- Waga, I., & Frieman, J.A. 2000, *Phys. Rev. D*, 62, 043521
- Young, T.R. 1994, Ph.D. thesis, Univ. of Oklahoma
- Ziaeeepour, H. 2000, *astro-ph/0002400*

### FIGURE CAPTIONS

Fig. 1.— Lines in the panels in the upper row show luminosity distance  $D_L(z, \alpha)$  as a function of redshift  $z$  for various values of  $\alpha$  computed for Hubble parameter  $H_0 = 65 \text{ km s}^{-1} \text{ Mpc}^{-1}$  for the spatially-flat time-variable  $\Lambda$  model with scalar field potential  $V(\phi) \propto \phi^{-\alpha}$ . In descending order at  $z = 2$  the lines correspond to  $\alpha = 0, 2, 4$ , and  $8$  (solid, dot-dashed, dashed, and dotted curves respectively).  $\alpha = 0$  is the constant  $\Lambda$  model. From left to right the three panels correspond to  $\Omega_0 = 0.2, 0.4$ , and  $0.6$ . The three lower panels show the fractional differences relative to the  $\alpha = 0$  case,  $1 - D_L(z, \alpha)/D_L(z, \alpha = 0)$ , as a function of  $z$ , for the values of  $\Omega_0$  used in the upper panels. Here the lines correspond to  $\alpha = 8, 4$ , and  $2$ , in descending order at  $z = 2$ .

Fig. 2.— Contours of  $N_\sigma = 1, 2, 4$ , and  $8$  for the constant  $\Lambda$  model. Left panel is for anticipated SNAP data with worst case errors, center panel is for neutral case errors, and right panel is for best case errors. The fiducial model is spatially-flat with  $\Omega_0 = 0.28$  and  $\Omega_\Lambda = 0.72$ .

Fig. 3.— Contours of  $N_\sigma = 1, 2, 4$ , and  $8$  for the spatially-flat time-variable  $\Lambda$  model (Peebles & Ratra 1988). Left panel is for anticipated SNAP data with worst case errors, center panel is for neutral case errors, and right panel is for best case errors. The fiducial model has  $\Omega_0 = 0.28$  and  $\alpha = 0$  (and is thus a constant  $\Lambda$  model with  $\Omega_\Lambda = 0.72$ ; this was also the fiducial model used for Fig. 2).

Fig. 4.— Contours of  $N_\sigma = 1, 2, 4$ , and  $8$  for the spatially-flat time-variable  $\Lambda$  model. Left panel is for anticipated SNAP data with worst case errors, center panel is for neutral case errors, and right panel is for best case errors. The fiducial model has  $\Omega_0 = 0.2$  and  $\alpha = 4$ .

Fig. 5.—  $N_\sigma(\Omega_0)$  for a flat model with a constant  $\Lambda$  (left panel) and for an open model with no  $\Lambda$  (right panel). In both cases the fiducial model has  $\Omega_0 = 0.3$ , with  $\Omega_\Lambda = 0.7$  and  $0$  respectively. Solid lines are for neutral case SNAP errors while dotted (dashed) lines are for best (worst) case ones.

Fig. 6.—  $N_\sigma(\Omega_0)$  (left panel) and  $N_\sigma(\alpha)$  (right panel) for the spatially-flat time-variable  $\Lambda$  model (Peebles & Ratra 1988). In both cases the fiducial model has  $\Omega_0 = 0.2$  and  $\alpha = 4$ . Solid lines are for neutral case SNAP errors while dotted (dashed) lines are for best (worst) case ones.

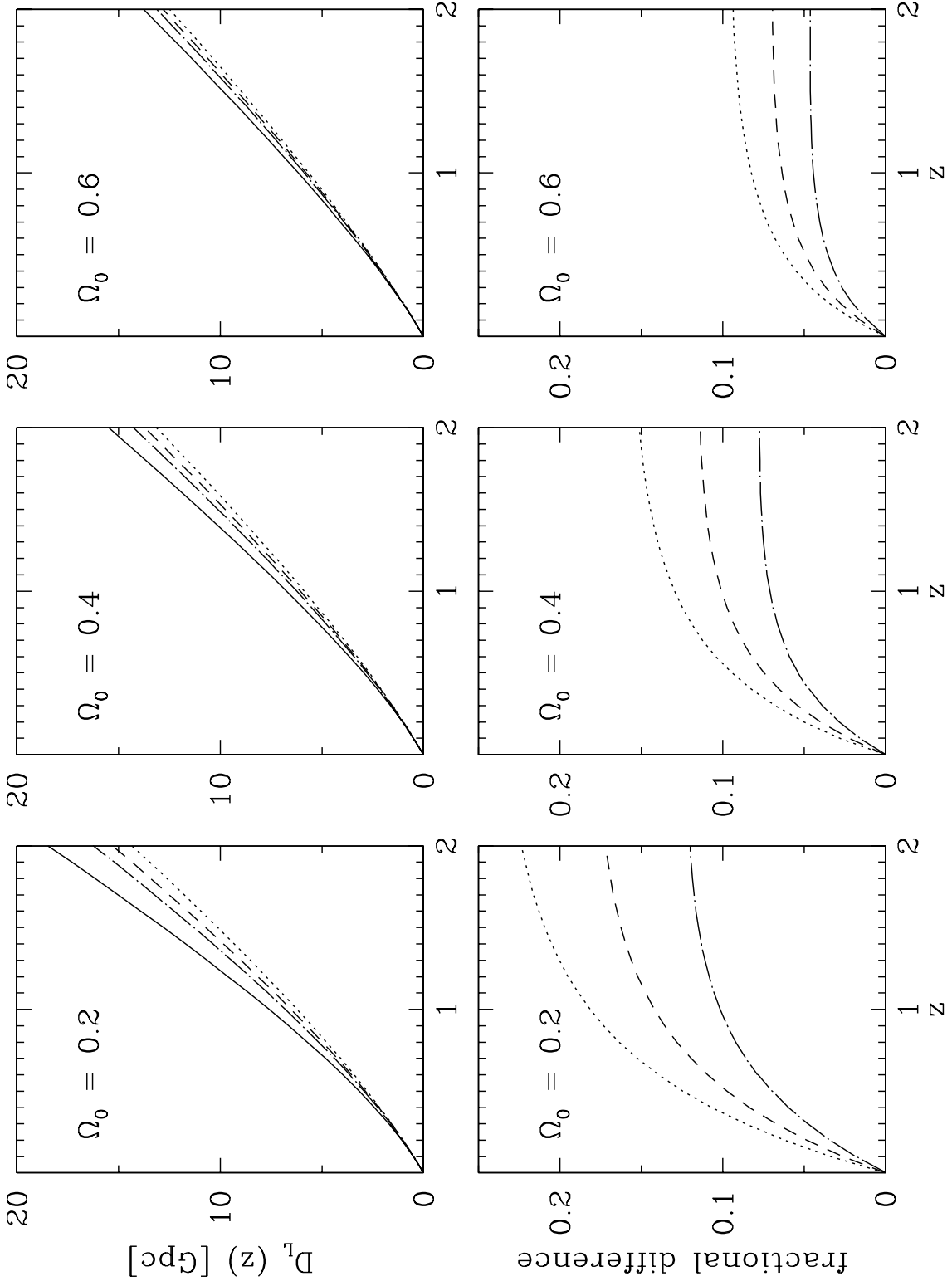


Figure 1

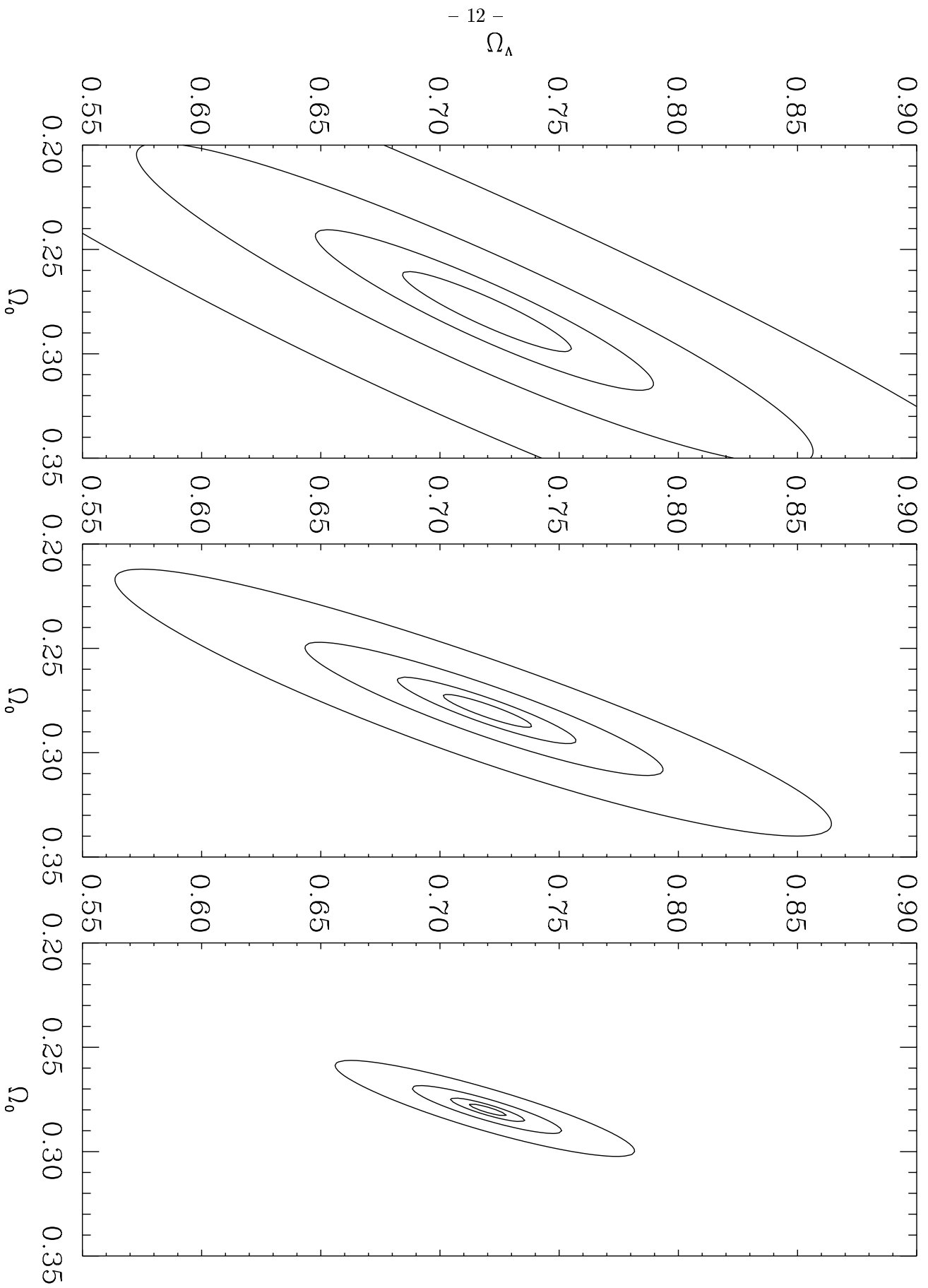


Figure 2

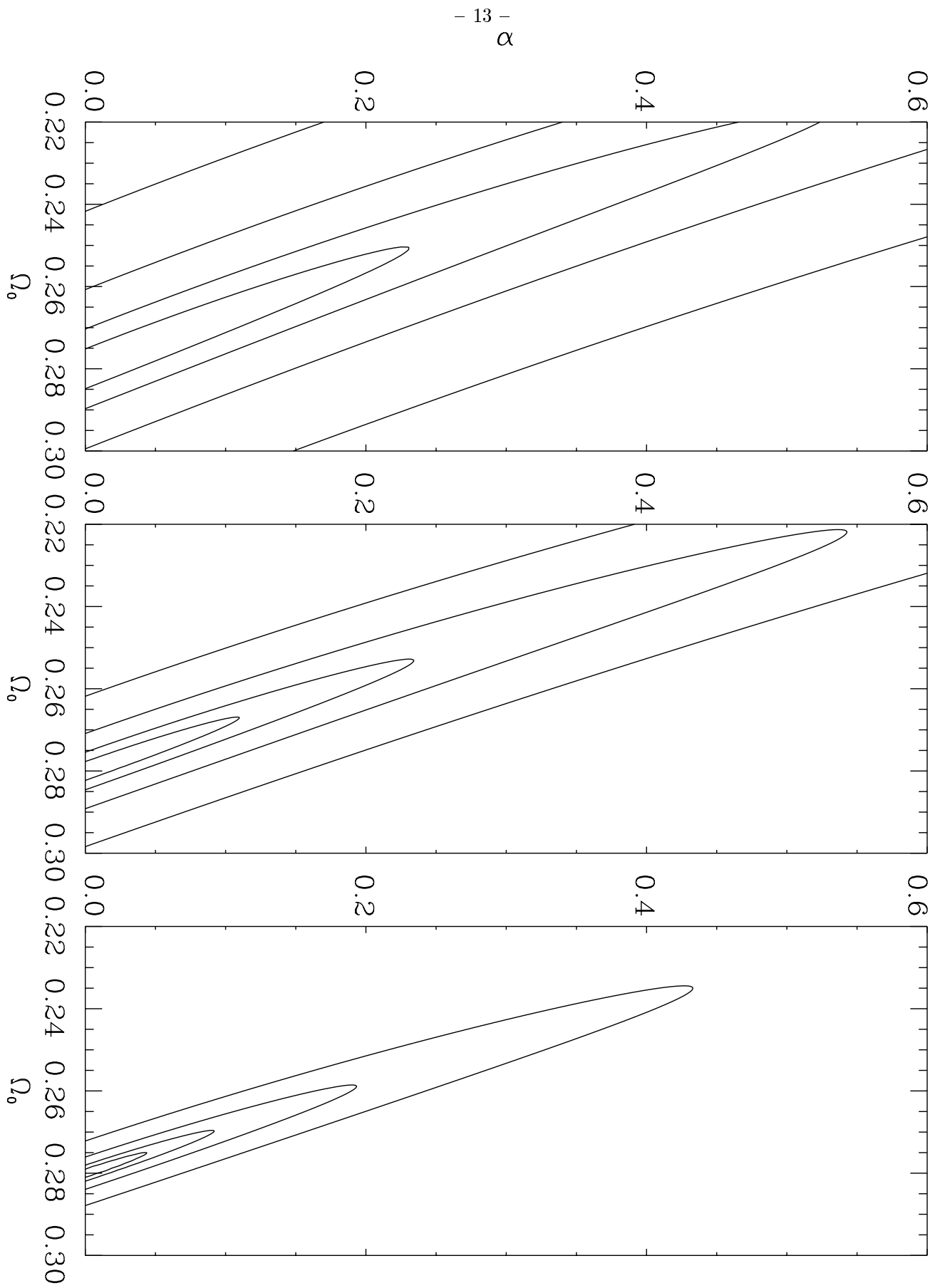


Figure 3

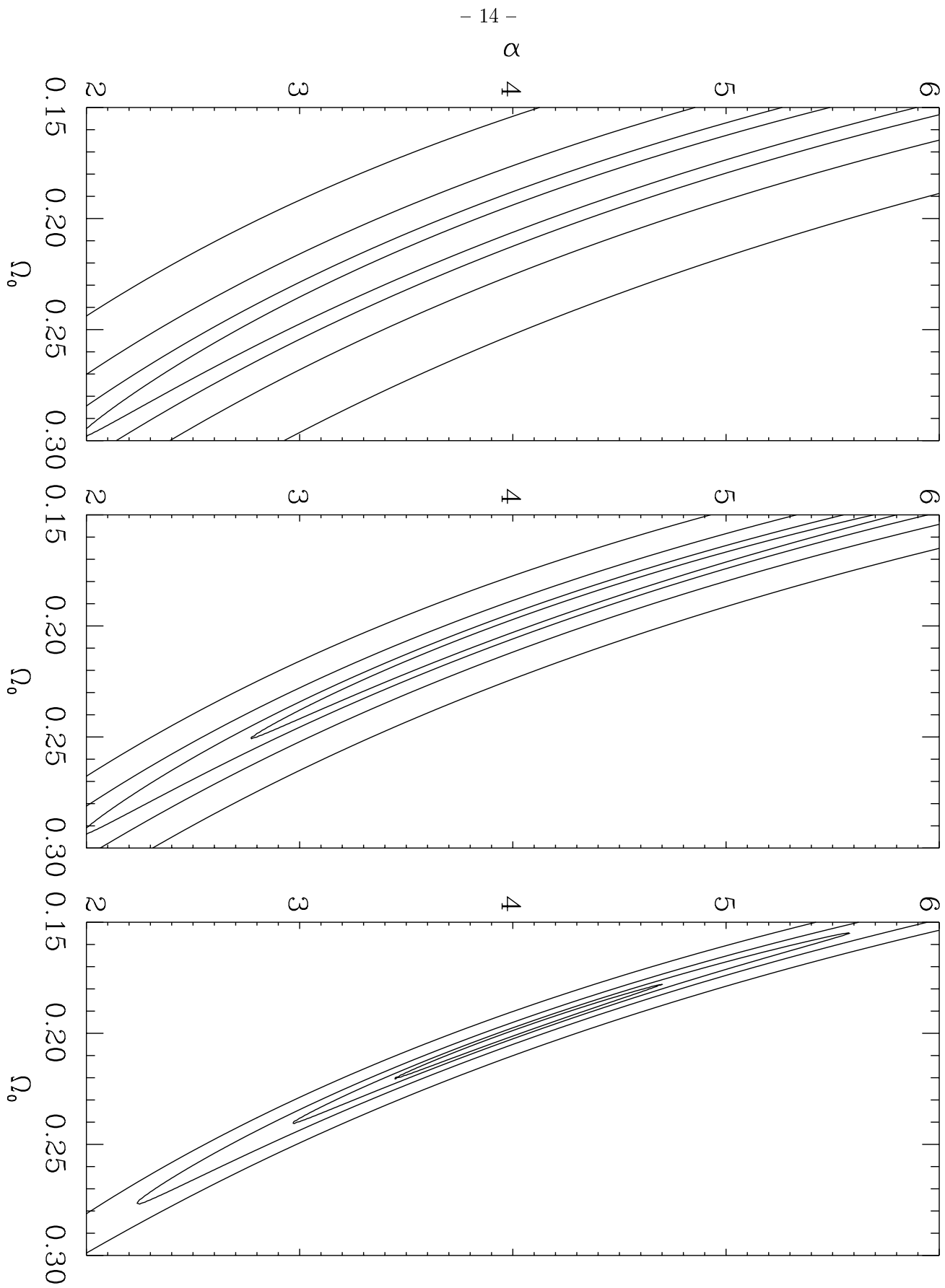


Figure 4

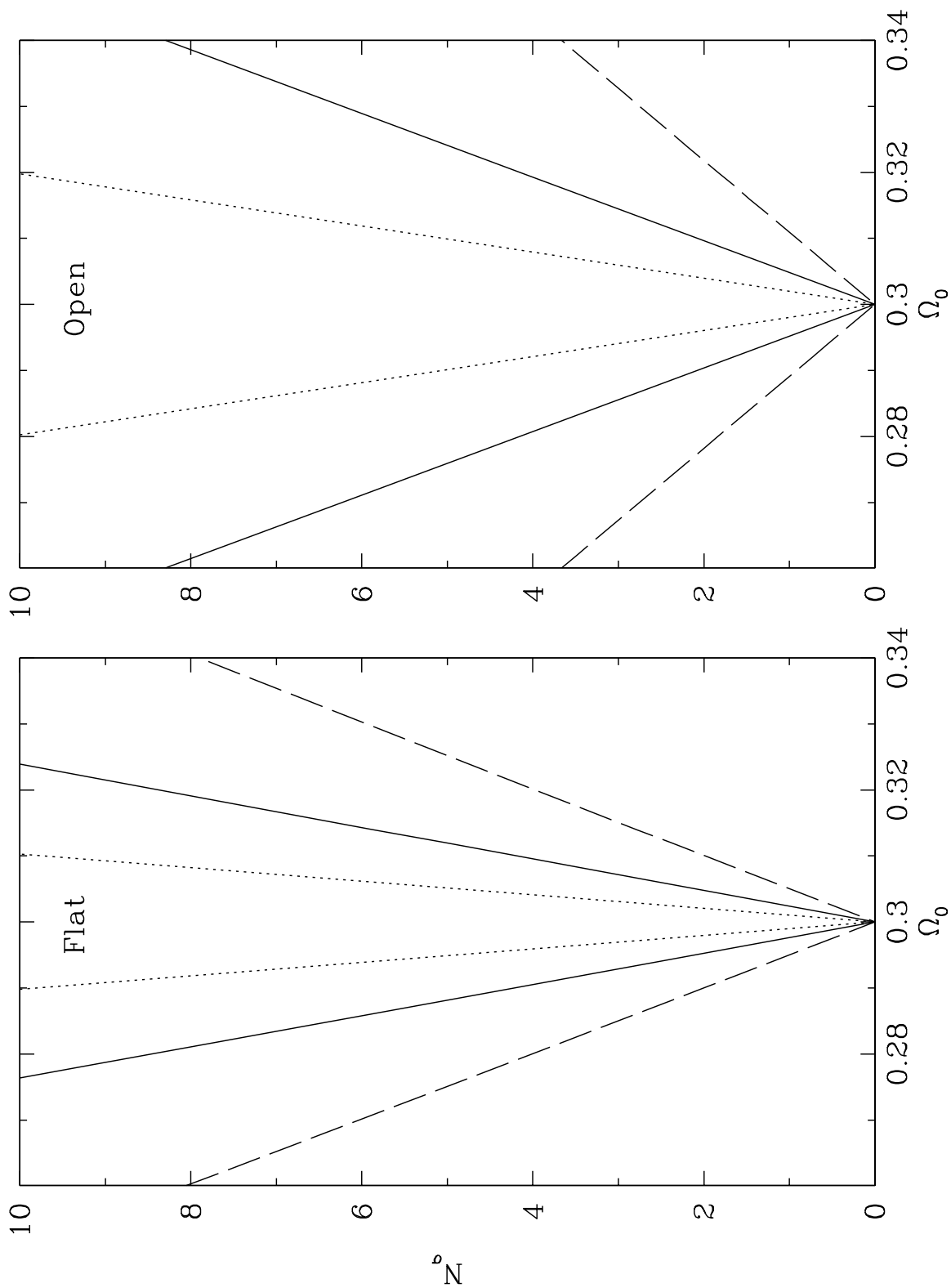


Figure 5

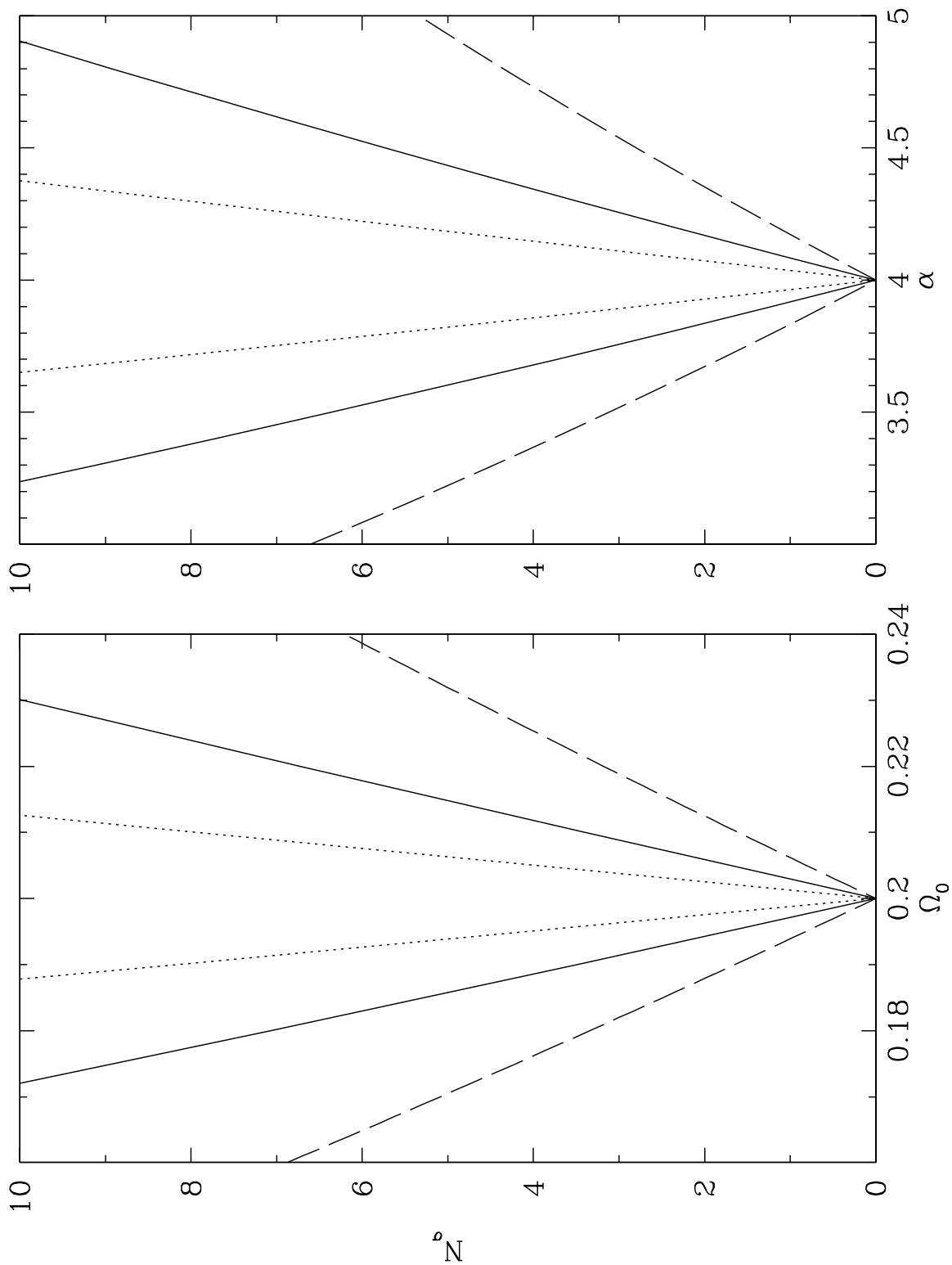


Figure 6